

Temperature Measurement of Semitransparent Silicon Wafers Based Upon Absorption Edge Wavelength Shift

T. Iuchi · T. Seo

Received: 3 March 2010 / Accepted: 30 June 2010 / Published online: 23 July 2010
© Springer Science+Business Media, LLC 2010

Abstract The temperature dependence of silicon wafer transmittance is well understood, and is caused by various absorption mechanisms over a wide spectral range. As the wavelength increases, the photon energy decreases until it becomes lower than the minimum energy gap in the silicon band structure. At this point, which is often referred to as the absorption edge wavelength, there is a rapid drop in absorption. The absorption edge shifts to a longer wavelength with increasing temperature, because the bandgap narrows with increasing temperature. Experiments were carried out with varying wavelength (900 nm to 1700 nm), polarization (p- and s-polarized), and direction (from normal to 80°), using specimens with different resistivities (0.01 Ω · cm to 2000 Ω · cm). A characteristic curve relating the absorption edge wavelength and temperature was obtained for all of the silicon wafers, despite their differing resistivity. This method enables *in situ* temperature measurements of silicon wafers from room temperature to 900 K, using wavelengths to which the wafer is semitransparent. In this article, an experimental apparatus and measurement results are described in detail, and several remaining problems are discussed.

Keywords Absorption edge wavelength · Bandgap energy · Silicon wafer · Transmittance

1 Introduction

The temperature measurement of a silicon wafer is important for the precise control of any thermally dependent manufacturing process. The difficulty of obtaining an accurate, reproducible measurement of wafer temperature, however, remains a principal

T. Iuchi (✉) · T. Seo
Toyo University, Kawagoe, Saitama 350-8585, Japan
e-mail: iuchi@toyonet.toyo.ac.jp

problem obstructing high-quality processing [1–3]. In semiconductor processing, non-contact temperature measurement of wafers is crucial, because it is contaminant-free. Radiation thermometry is a typical method meeting this requirement [4], but its accuracy is limited by the uncertainty in the emissivity of the silicon wafer and the thin film layers deposited on the wafer, such as oxide films. The radiative properties of silicon wafers are complex, and change during processing [4–9]. In order to overcome this problem, we developed a radiation thermometry method that enables the simultaneous measurement of emissivity and temperature of a silicon wafer, based upon a polarization technique [10]. This method is, however, limited to relatively high temperatures above 900 K, at which the wafers are opaque. We are currently investigating an alternative non-contact measurement method that can be used at relatively low temperatures with semitransparent silicon wafers.

The temperature dependence of the wafer transmittance is well understood. There are various absorption mechanisms over a wide spectral range [5, 7, 11–14]. As the wavelength increases, the photon energy decreases until it becomes lower than the minimum energy gap in the silicon band structure. At this point, there is a rapid drop in absorption, which is often referred to as the absorption edge wavelength λ_e . This edge shifts to a longer wavelength with increasing temperature, because the bandgap narrows with increasing temperature.

We designed a measurement system to determine the relationship between the absorption edge wavelength and temperature. Experiments were carried out at various wavelengths ($\lambda = 900 \text{ nm}$ to 1700 nm), polarizations (p- and s-polarized), and directions ($\theta = \text{normal to } 80^\circ$), on specimens with various resistivities ($\rho = 0.01 \Omega \cdot \text{cm}$ to $2000 \Omega \cdot \text{cm}$) that corresponded with different impurity concentrations doped into a silicon wafer. A characteristic curve relating the absorption edge wavelength and temperature of a silicon wafer was obtained. Once the absorption edge wavelength was measured, the temperature was uniquely determined from this relationship. In this article, an experimental system and measurement results are described in detail, and several remaining problems are discussed.

2 Experimental Apparatus

Figure 1 shows an experimental system with a heating furnace in vacuum for transmittance measurements of a silicon wafer. Figure 2 shows a photograph of this experimental system. A collimated light beam originating from a tungsten–krypton bulb (SL-1, StellarNet) and delivered through an optical fiber was irradiated upon a silicon wafer (20 mm in diameter) inside the vacuum furnace. After the light transmitted through the silicon wafer was divided into polarized components by a polarizer (10LP-NIR, New Port), it arrived at a monochromator, and was detected by InGaAs array sensors (EPP2000-NIR-InGaAs 512, StellarNet). Spectral radiance signals from 900 nm to 1700 nm were processed. The temperature of the furnace was measured by a K-type thermocouple embedded in a silicon wafer for temperature calibration of the specimen location in the furnace, as shown in Fig. 1. The size of the thermocouple-embedded silicon wafer was the same as that of the specimen wafer. The specimen temperature was assumed to be the same as the temperature reading from the embedded thermocouple,

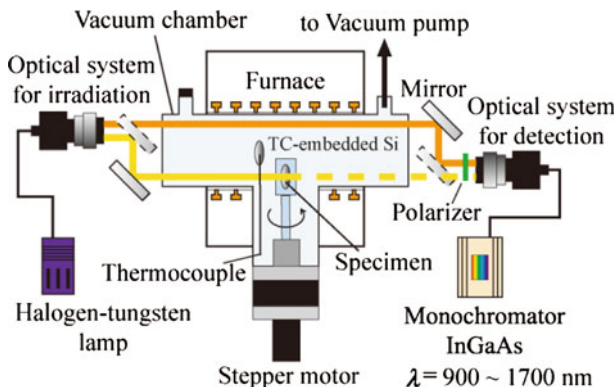


Fig. 1 Experimental system with a heating furnace in vacuum for transmittance measurement of a silicon wafer

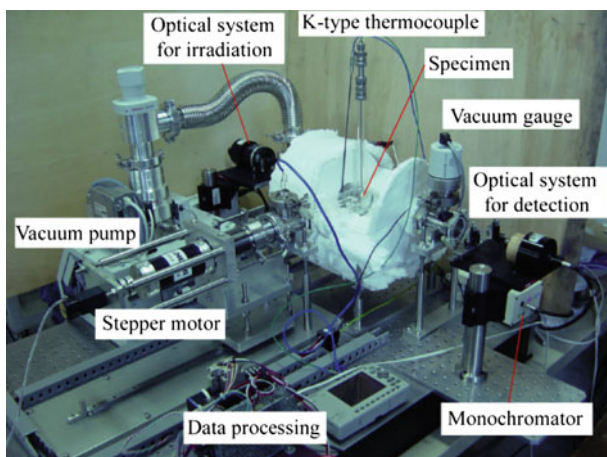


Fig. 2 Photograph of the experimental system

because thermal equilibrium was maintained in the furnace. The distance between the optical systems for irradiation and detection was about 600 mm.

The transmittance τ of a silicon wafer at temperature T in the furnace was calculated by the following equation:

$$\tau = \frac{E_t - E_n}{E_r - E_n} \quad (1)$$

where E_t is the transmitted radiance signal through the silicon wafer, E_r the reference radiance signal not transmitted through the silicon wafer, and E_n the noise radiance in the furnace.

In this study, an absorption edge wavelength λ_e is defined as a wavelength when the transmittance τ reached 0.01. Figure 3 shows the procedure used to measure the

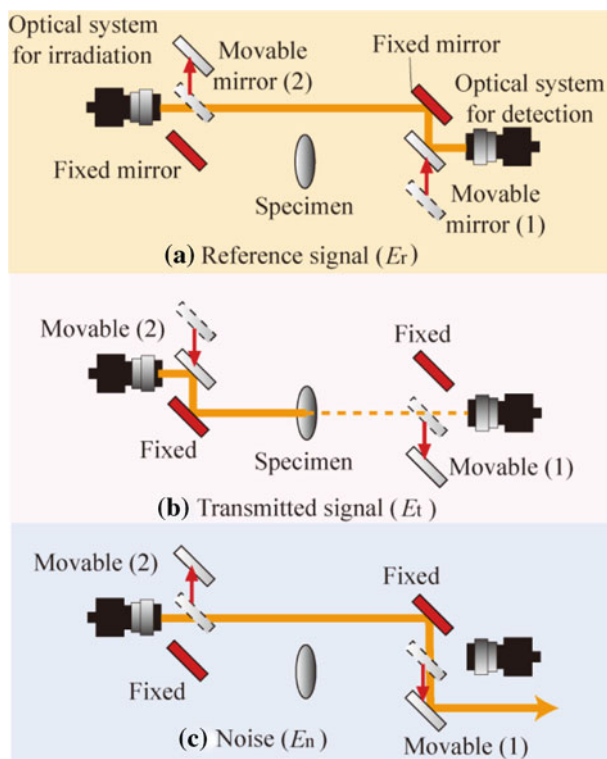


Fig. 3 Double beam optical system for the transmittance measurement

transmittance τ using a double beam optical system, where E_r , E_t , and E_n were measured by the mirror arrangements shown in (a), (b), and (c), respectively.

3 Measurements

Table 1 lists sample specifications and measurement conditions. Table 2 shows the relationship between the resistivity and impurity concentration doped in a silicon wafer [15].

Several experiments were carried out to determine the general behavior of the silicon wafers in connection with the temperature, wavelength, resistivity, polarization, and direction.

Figure 4 shows the experimentally determined relationship between the temperature T and spectral transmittance τ for a silicon wafer with a resistivity of $\rho = 1 \Omega \cdot \text{cm}$. Similarly, Fig. 5 shows experimental results demonstrating the onset of an absorption edge wavelength λ_e for the same specimen used in Fig. 4. It is clear from Figs. 4 and 5 that the transmittance τ decreased with increasing temperature T , and the absorption edge wavelength λ_e shifted to a longer wavelength with increasing T . At 1073 K, the transmittance essentially became zero.

Table 1 Specifications of specimens and measurement conditions

Specimen
N type silicon wafer
Orientation: (100)
Dimensions: thickness $t = (0.5, 0.75, 2.0)$ mm, diameter = 20 mm
Resistivity: $\rho = (0.01, 0.1, 1.0, 60, 2000)$ $\Omega \cdot \text{cm}$
Oxide film thickness (SiO_2): $d = (0 \text{ (bare)}, 200, 350, 550, 750 \text{ and } 950)$ nm
Surface condition: roughness $R_a = 0.03 \mu\text{m}$ (specular)
Measurement conditions
Wavelength: $\lambda = 900 \text{ nm to } 1700 \text{ nm}$
Polarization: p- and s-polarized components
Direction: 0° to 80° (from the normal to the surface)
Temperature: $T = 300 \text{ K to } 1073 \text{ K}$
Atmosphere: in air and in vacuum ($\sim 10^{-3} \text{ Pa}$)

Table 2 Relationship between impurity concentration and resistivity of silicon wafers at room temperature [15]

Resistivity, ρ ($\Omega \cdot \text{cm}$)	Impurity concentration (cm^{-3})
0.01	$\sim 8 \times 10^{19}$
1	$\sim 6 \times 10^{15}$
2000	$\sim 3 \times 10^{14}$

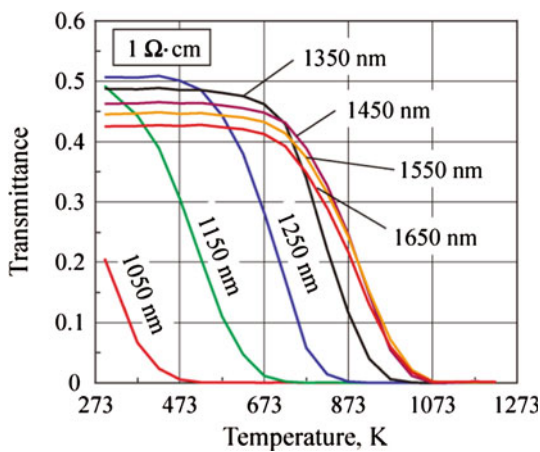
Fig. 4 Experimental relations between temperature T and spectral transmittance τ for a silicon wafer with $\rho = 1 \Omega \cdot \text{cm}$ at 0° (wavelength as a parameter)

Figure 6 shows the experimentally determined directional polarized transmittance τ of a silicon wafer with a resistivity of $\rho = 1 \Omega \cdot \text{cm}$ at $\lambda = 1550 \text{ nm}$ in the temperature range between 300 K and 1073 K, for (a) p-polarization and (b) s-polarization. A characteristic pattern of polarized transmittance was clearly observed. Both p- and

Fig. 5 Experimental relations between wavelength λ and transmittance τ for a silicon wafer with $\rho = 1 \Omega \cdot \text{cm}$ at 0° (temperature as a parameter)

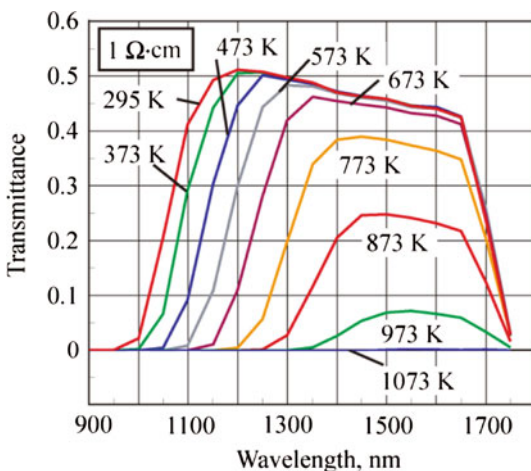


Fig. 6 Experimental results of directional polarized transmittance τ for a silicon wafer with $\rho = 1 \Omega \cdot \text{cm}$ at $\lambda = 1550 \text{ nm}$ at $\theta = 0^\circ$ to 80° and $T = 300 \text{ K}$ to 1073 K (temperature as a parameter):
(a) p-polarized and
(b) s-polarized

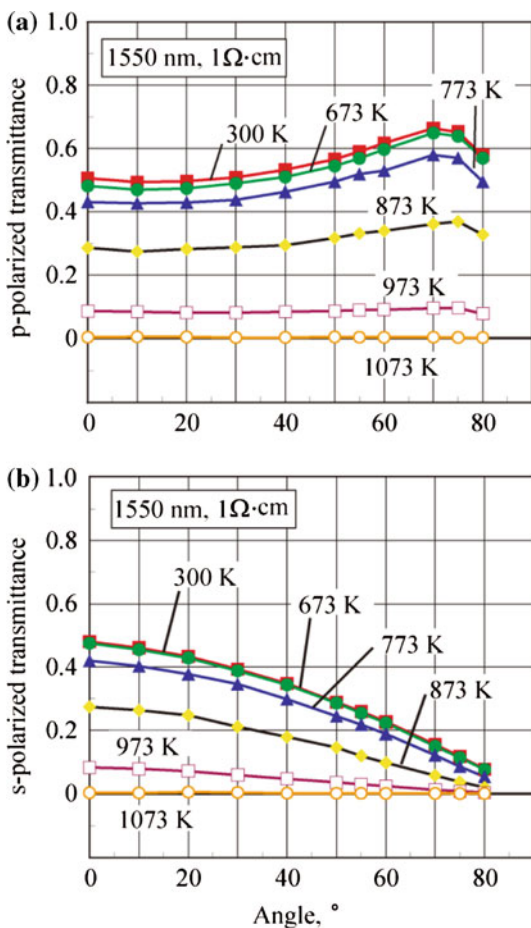
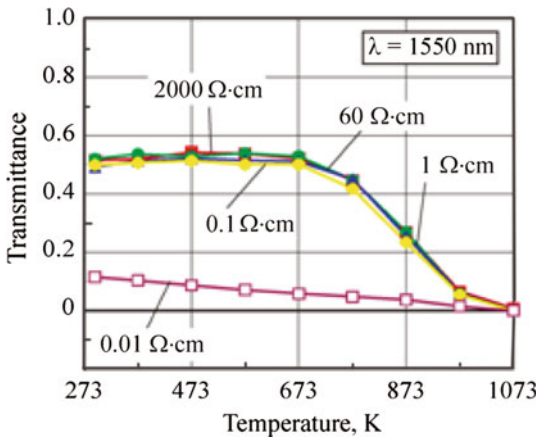


Fig. 7 Experimental relations between temperature T and transmittance τ of silicon wafers with different resistivity ρ at $\theta = 0^\circ$ and $\lambda = 1550$ nm (resistivity as a parameter)



s-polarized transmittance decreased with increasing temperature, finally disappearing at 1073 K.

Figure 7 shows the experimental relationship between the temperature T and transmittance τ of silicon wafers with different resistivities at $\lambda = 1550$ nm. The curves representing the temperature dependence τ for most wafers overlapped, but the wafer with $\rho = 0.01 \Omega \cdot \text{cm}$ was so heavily doped with impurities that electromagnetic waves penetrating the substrate interacted with electrons, resulting in a large reduction of transmittance.

Figure 8 shows the experimental relationship between the direction θ and absorption edge wavelength λ_e of a silicon wafer with $1 \Omega \cdot \text{cm}$ and the effect of polarization. λ_e for p-polarization at a specified temperature remained constant independent of the direction θ , while λ_e for s-polarization moved to longer wavelengths with increasing angle θ . This phenomenon was caused by a decrease in s-polarized transmittance at large angles, as shown in Fig. 6b.

Figure 9 shows experimental results demonstrating the effect of oxide film thickness d on absorption edge wavelength. This phenomenon may have been caused by an interference effect due to multiple reflections of radiation between the surfaces of the oxide film and the silicon wafer.

Similarly, Fig. 10 shows the effect of the wafer thickness t on the absorption edge wavelength λ_e , which shifted to longer wavelengths with increasing thickness t . This was caused by a decrease in transmittance with increasing t . Therefore, the thickness change must be compensated for in the measurement of the absorption edge wavelength.

Based on these experimental results, many additional experiments were performed to determine a quantitative relationship between the temperature and absorption edge wavelength.

Figure 11 shows this experimental relationship between the temperature T and absorption edge wavelength λ_e in the temperature range from 300 K to 900 K at $\theta = 0^\circ$, with silicon wafers of resistivity ρ from $0.1 \Omega \cdot \text{cm}$ to $2000 \Omega \cdot \text{cm}$. This relationship

Fig. 8 Experimental relations between direction θ and absorption edge wavelength λ_e of a silicon wafer with $\rho = 1 \Omega \cdot \text{cm}$ (temperature as a parameter): (a) p-polarized and (b) s-polarized

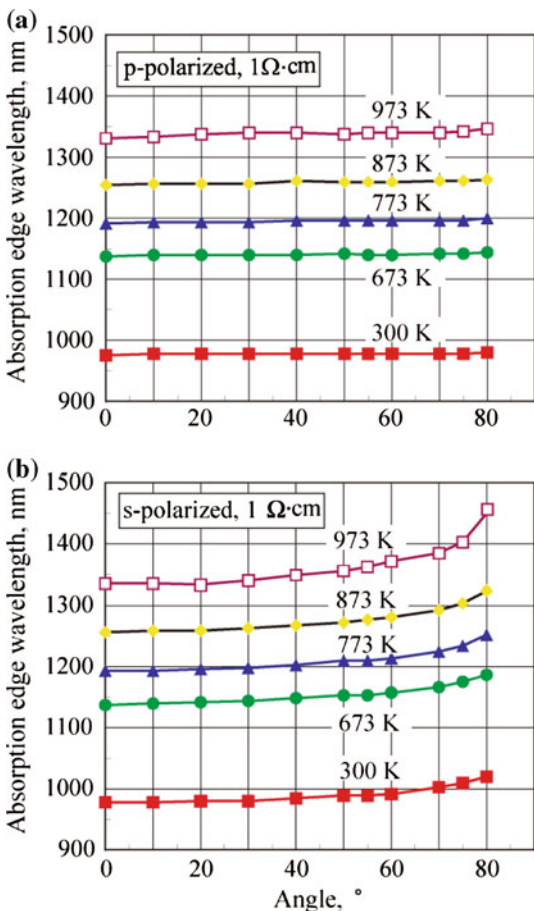


Fig. 9 Experimental relations between oxide film thickness d and absorption edge wavelength λ_e of silicon wafers with $\rho = 1 \Omega \cdot \text{cm}$ at $\theta = 0^\circ$ (temperature as a parameter)

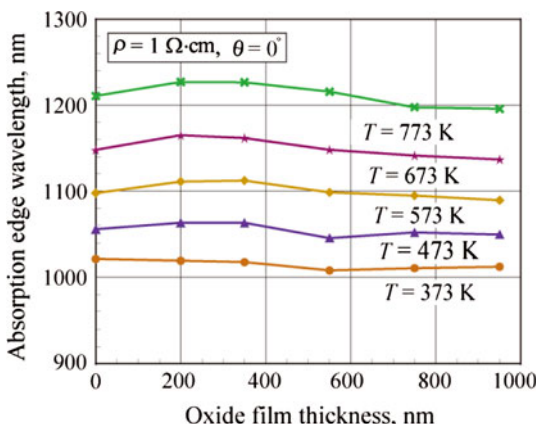


Fig. 10 Experimental relations between wafer thickness t and absorption edge wavelength λ_e for a wafer with $\rho = 1 \Omega \cdot \text{cm}$ at $\theta = 0^\circ$ and $T = 300 \text{ K}$

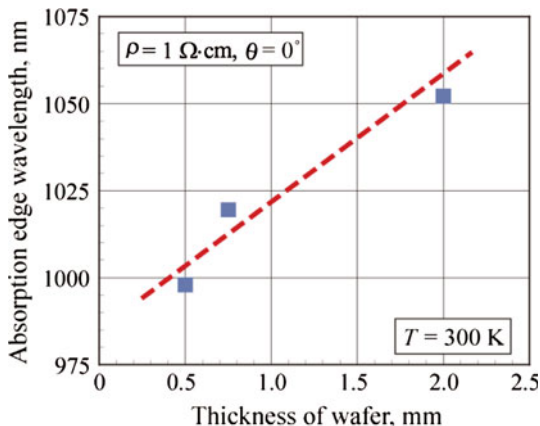
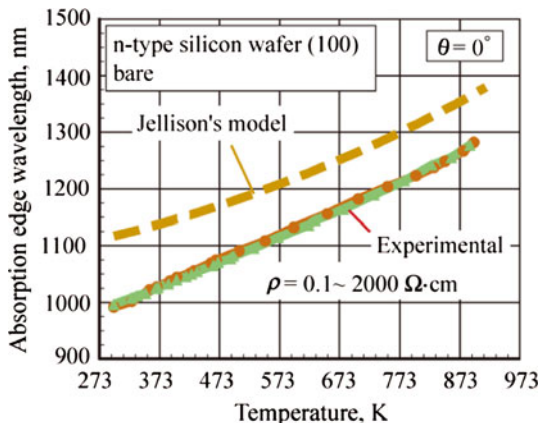


Fig. 11 Experimental relation ($T-\lambda_e$ relation) between temperature T and absorption edge wavelength λ_e of silicon wafers with $\rho = 0.1 \Omega \cdot \text{cm}$ to $2000 \Omega \cdot \text{cm}$ at $\theta = 0^\circ$ and the comparison with Jellison's model



was named the $T-\lambda_e$ relation. As a consequence, once the absorption edge wavelength is measured, the temperature of a silicon wafer can be uniquely determined.

The absorption edge wavelength λ_e was originally defined as [15]

$$\lambda_e = \frac{1.24 \times 10^3}{E_g} [\text{nm}] \quad (2)$$

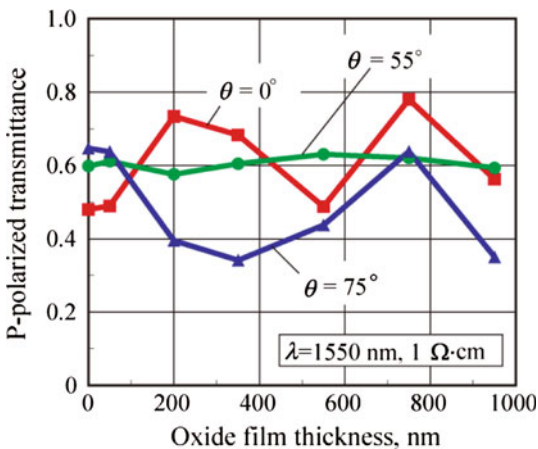
where E_g is the bandgap energy in eV of a semiconductor. E_g of a silicon wafer is 1.12 eV at room temperature, and decreases with increasing temperature.

According to Jellison's model [16], the bandgap energy $E_g(T)$ of the silicon wafer in Eq. 2 is expressed in the following equation as a function of temperature T :

$$E_g(T) = E_g(0) - \frac{AT^2}{B + T} \quad (3)$$

where $A = 4.73 \times 10^{-4} \text{ eV} \cdot \text{K}^{-1}$, $B = 635 \text{ K}$, and $E_g(0) = 1.155 \text{ eV}$.

Fig. 12 Experimental relations between oxide film thickness d and p-polarized transmittance τ of silicon wafers with $\rho = 1 \Omega \cdot \text{cm}$ at $\lambda = 1550 \text{ nm}$ where $\theta = 0^\circ, 55^\circ$, and 75°



The absorption edge wavelength λ_e according to Jellison's model was calculated using Eqs. 2 and 3, and these are depicted in Fig. 11. There was a difference of about 100 nm between the λ_e 's from Jellison's model and the authors' experimental results.

Figure 12 shows experimental relationships between the oxide film thickness d and p-polarized transmittance τ of silicon wafers ($\rho = 1 \Omega \cdot \text{cm}$) at $\lambda = 1550 \text{ nm}$ for angles $\theta = 0^\circ, 55^\circ$, and 75° . The transmittance τ remained unchanged at $\theta = 55^\circ$ independent of the wide changes in oxide film thickness, while τ seemed to periodically change with increasing film thickness at 0° and 75° . Therefore, the p-polarized transmittance at $\theta = 55^\circ$ is a good choice for the measurement of the absorption edge wavelength, because variation of the oxide film thickness does not affect the measurement. The angle of 55° is the Brewster angle between the oxide film (SiO_2) and air.

4 Conclusions

A non-contact temperature measurement technique for silicon wafers, based on the shift of the absorption edge wavelength under various conditions such as impurity doping concentration, oxide film thickness, wafer thickness, and polarization, was investigated in vacuum and in air at temperatures ranging from 300 K to 1073 K.

The following conclusions were reached:

- (1) An experimental relationship between the temperature T and absorption edge wavelength λ_e (a $T-\lambda_e$ relation) was obtained for silicon wafers with a resistivity greater than $\rho = 0.1 \Omega \cdot \text{cm}$, and for temperatures between 300 K and 900 K at which Si wafers are semitransparent. From this relationship, the temperature of a silicon wafer can be determined from the measurement of λ_e .
- (2) The precise measurement of the absorption edge wavelength of silicon wafers with a resistivity less than $\rho = 0.01 \Omega \cdot \text{cm}$ is difficult because of their low transmittance.

- (3) The thickness t of a silicon wafer affects the measurement of λ_e . Therefore, in general, one must correct for any variation in t .
- (4) P-polarization is preferable for measuring λ_e of silicon wafers with oxide films. Furthermore, measuring the p-polarized transmittance at $\theta = 55^\circ$ enables the measurement of λ_e without any oxide film thickness variation effect.
- (5) The experimentally obtained λ_e was shorter by about 100 nm than that obtained from Jellison's model. This problem remains unsolved.
- (6) The uncertainty in temperature measurement using the $T-\lambda_e$ relation has not yet been analyzed. This will be a high-priority future investigation.
- (7) The background radiation noise from heating sources should be avoided when applying the $T-\lambda_e$ relationship to a real process. This problem is currently under investigation.

Acknowledgments The authors express their thanks to R. Shinagawa for his contributions to this study during his time as a graduate student at Toyo University. The present research was supported in part by the Ministry of Education, Science, Sports and Culture through a Grand-in-Aid for Scientific Research (C) (Project Number 20560403) and as a "High-Tech Research Center" Project for Private Universities through matching funds from the Ministry of Education, Sports, Science, and Technology, 2004–2008.

References

1. B.E. Adams, C.W. Schietinger, K.G. Kreider, in *Radiometric Temperature Measurements II Applications*, ed. by Z.M. Zhang, B.K. Tsai, G. Machin (Academic Press, Amsterdam, 2009)
2. R.L. Anderson, in *Temperature: Its Measurement and Control in Science and Industry*, vol. 6, part 2, ed. by J.F. Schooley (AIP, New York, 1992), pp. 1117–1122
3. B.E. Adams, in *Proceedings of TEMPMEKO '99, 7th International Symposium on Temperature and Thermal Measurement in Industry and Science*, ed. by J.F. Debbeldam, M.J. de Groot (Edauw Johannissen bv, Delft, 1999), pp. 1–10
4. R. Siegel, J.R. Howell, in *Thermal Radiation Heat Transfer*, 3rd edn. (Taylor & Francis, Philadelphia, 1992)
5. T. Sato, Jpn. J. Appl. Phys. **6**, 339 (1967)
6. P. Vandenabeele, K. Maex, SPIE **1393**, 316 (1990)
7. P.J. Timans, J. Appl. Phys. **74**, 6353 (1993)
8. B. Adams, C. Schietinger, in *Temperature: Its Measurement and Control in Science and Industry*, vol. 7, part 2, ed. by D.C. Ripple (AIP, New York, 2002), pp. 1081–1086
9. P.J. Timans, in *Advances in Rapid Thermal and Integral Processing*, ed. by F. Roozeboom (Kluwer Academic Publishers, Dordrecht, Netherlands, 1996), pp. 35–101
10. T. Iuchi, A. Gogami, in *XIX IMEKO World Congress* (Lisbon, Portugal 2009), pp. 1487–1492
11. H. Rogne, P.J. Timan, H. Ahmed, Appl. Phys. Lett. **69**, 2190 (1996)
12. J.C. Sturm, P.V. Schwartx, P.M. Garone, Appl. Phys. Lett. **56**, 961 (1990)
13. M.E. Adel, Y.I. Shalom, S. Mangan, D. Cabib, SPIE **1803**, 290 (1992)
14. J.C. Sturm, C.M. Reaves, IEEE Trans. Electron Devices **39**, 81 (1992)
15. S.M. Sze, in *Semiconductor Devices, Physics and Technology*, 2nd edn. (Wiley, New York, 2002)
16. G.E. Jellison, D.H. Lowndes, Appl. Phys. Lett. **4**, 594 (1982)